

Modeling of 1D elastic P-waves in a fractured rock with hyperbolic jump conditions

B. Lombard^{†,*}, J. Piraux^{†,*}

[†]Laboratoire de Mécanique et d'Acoustique, 13402 Marseille, FRANCE

*Email: lombard@lma.cnrs-mrs.fr

Abstract

We numerically investigate the elastic wave propagation inside a 1D fractured rock, in the time-domain. The dry fracture is described by a nonlinear model used in geo-mechanics. To take into account the jump conditions on a regular grid, the finite-difference schemes are coupled with an interface method. Numerical experiments show that the nonlinear effects tend to sharpen the profiles of waves.

1 Introduction

We study the one-dimensional propagation of compressional waves in a fractured rock. The rock is linearly elastic, with a static stress $-\bar{\sigma}$ ($\bar{\sigma} > 0$). The wavelengths of perturbations are supposed to be much larger than the thickness of the dry fracture (h with perturbations, \bar{h} without), so that the fracture is replaced by an interface at $x = \alpha$ (figure 1). The jump conditions are deduced from a classical model in geomechanics, the hyperbolic model of Bandis-Barton [1], which describes the nonlinear deformations of asperities in terms of the applied stresses.

The goal of our work is to develop numerical methods to study this configuration in the time-domain. To our knowledge, only [7] has addressed wave propagation across a fracture described by the Bendis-Barton model, with the method of characteristics. Our approach is based on classical finite-difference schemes and on an interface method previously developed for linear contacts [3], [4], [5].

2 Problem statement

2.1 Conservation laws

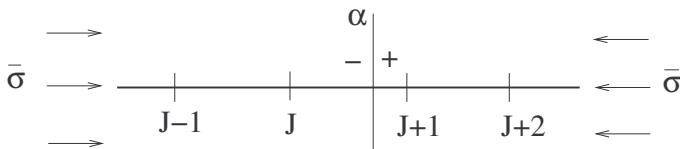


Figure 1: 1D rock fractured at $x = \alpha$; spatial mesh.

The density ρ and the elastic speed of P-waves c are

$$(\rho, c) = \begin{cases} (\rho_0, c_0) & \text{if } x < \alpha \\ (\rho_1, c_1) & \text{if } x > \alpha. \end{cases} \quad (1)$$

Outside α , the linearization of mechanics equations around the pre-stressed state leads to the equations

$$\frac{\partial v}{\partial t} = \frac{1}{\rho} \frac{\partial \sigma}{\partial x}, \quad \frac{\partial \sigma}{\partial t} = \rho c^2 \frac{\partial v}{\partial x}, \quad (2)$$

where $u, v = \frac{\partial u}{\partial t}$, and σ are perturbations of elastic displacement, of elastic velocity, and of elastic stress.

2.2 Jump conditions

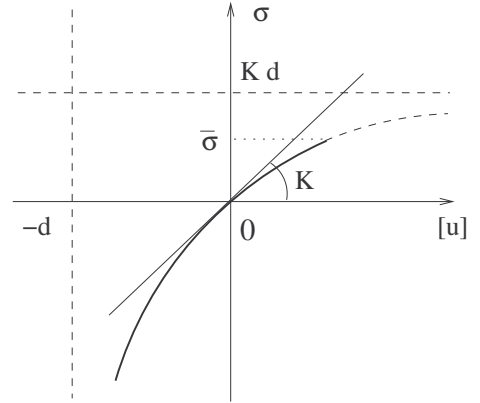


Figure 2: hyperbolic model of Bandis-Barton.

The Bandis-Barton model (hyperbola on figure 2) relies on two constants $K > 0$, $d > 0$, called the normal stiffness and the maximum allowable closure of the fracture, deduced from experimental measurements [1]. Setting $[f(\alpha, t)] = f(\alpha^+, t) - f(\alpha^-, t)$, the jump conditions are

$$\begin{aligned} [\sigma(\alpha, t)] &= 0, \\ [u(\alpha, t)] &= \frac{1}{K} \frac{\sigma(\alpha^-, t)}{1 - \frac{\sigma(\alpha^-, t)}{Kd}}. \end{aligned} \quad (3)$$

In compression ($\sigma < 0$), the second equation of (3) implies that $h \geq \bar{h} - d$: there is a limit in the compressibility of the fracture. In traction ($\sigma > 0$), the second equation

of (3) is realistic up to $\sigma = \bar{\sigma}$; above, the perturbations disconnect the sides of the fracture. In the limit of small movements, or if $d \gg \sigma(\alpha^-, t)/K$, we recover the linear condition [6] (tangent to the hyperbola on figure 2)).

We differentiate the second equation of (3) in terms of t and we replace the time derivative by a spatial derivative via (2)

$$\begin{aligned} \sigma(\alpha^+, t) &= \sigma(\alpha^-, t), \\ v(\alpha^+, t) &= v(\alpha^-, t) \\ &+ \frac{\rho_0 c_0^2}{K} \frac{1}{\left(1 - \frac{\sigma(\alpha^-, t)}{Kd}\right)^2} \frac{\partial v}{\partial x}(\alpha^-, t). \end{aligned} \quad (4)$$

Note that these zero-th order conditions involve a first-order derivative $\frac{\partial v}{\partial x}$. Similar differentiations are applied ($m - 1$) times on (4). Setting $\mathbf{U} = {}^T(v, \sigma)$, we get the m -th order jump conditions

$$\frac{\partial^m \mathbf{U}}{\partial x^m}(\alpha^+, t) = \mathbf{f}_m \left(\mathbf{U}, \dots, \frac{\partial^m \mathbf{U}}{\partial x^m}, \frac{\partial^{m+1} \mathbf{U}}{\partial x^{m+1}} \right) (\alpha^-, t), \quad (5)$$

where \mathbf{f}_m is a system of two nonlinear equations.

3 Numerical methods

3.1 Numerical scheme

Given $(x_i, t_n) = (i \Delta x, n \Delta t)$, where Δx is the mesh size and Δt is the time step, we seek an approximation \mathbf{U}_i^n of $\mathbf{U}(x_i, t_n)$. We use two-step, explicit, and $(2s + 1)$ -point spatially-centered finite-difference schemes. Time-stepping is written symbolically via the discrete operator \mathbf{H}

$$\mathbf{U}_i^{n+1} = \mathbf{U}_i^n + \mathbf{H}(\mathbf{U}_{i-s}^n, \dots, \mathbf{U}_{i+s}^n). \quad (6)$$

As observed in numerical experiments, sharp fronts can appear when nonlinear effects induced by the fracture are non negligible, even for smooth initial data. Consequently, it is interesting to use schemes which behave well with shock waves. To do so, we use a second-order scheme with flux limiter [2], issued from computational fluid mechanics ($s = 2$, stable up to CFL=1).

We define J so that $x_J \leq \alpha < x_{J+1}$ (figure 1). A grid point is *regular* if its time-stepping does not cross the interface; then, (6) is applied classically. Otherwise, a grid point is *irregular*. The irregular points are $x_{J-s+1}, \dots, x_{J+s}$.

3.2 Interface method

At irregular points, some numerical values used for time-stepping (6) are modified. These *modified values* are

computed and used as follows [3], [5]. On each side of α , we define a smooth extension $\mathbf{U}^*(x, t_n)$ of $\mathbf{U}(x, t_n)$ on the other side of α

$$\begin{aligned} x > \alpha, \mathbf{U}^*(x, t_n) &= \sum_{m=0}^{2k-1} \frac{(x - \alpha)^m}{m!} \frac{\partial^m \mathbf{U}}{\partial x^m}(\alpha^-, t_n), \\ x \leq \alpha, \mathbf{U}^*(x, t_n) &= \sum_{m=0}^{2k-1} \frac{(x - \alpha)^m}{m!} \frac{\partial^m \mathbf{U}}{\partial x^m}(\alpha^+, t_n). \end{aligned} \quad (7)$$

The modified value \mathbf{U}_i^* is a numerical estimation of $\mathbf{U}^*(x_i, t_n)$. The time-stepping at a irregular point x_i is

$$J - s + 1 \leq i \leq J,$$

$$\mathbf{U}_i^{n+1} = \mathbf{U}_i^n + \mathbf{H}(\mathbf{U}_{i-s}^n, \dots, \mathbf{U}_J^n, \mathbf{U}_{J+1}^*, \dots, \mathbf{U}_{i+s}^*)$$

$$J + 1 \leq i \leq J + s,$$

$$\mathbf{U}_i^{n+1} = \mathbf{U}_i^n + \mathbf{H}(\mathbf{U}_{i-s}^*, \dots, \mathbf{U}_J^*, \mathbf{U}_{J+1}^n, \dots, \mathbf{U}_{i+s}^n). \quad (8)$$

To estimate the limit values in (7), we write Taylor expansions of $\mathbf{U}(x_i, t_n)$ "on the left" of α ($i = J - k + 1, \dots, J$)

$$\mathbf{U}(x_i, t_n) = \sum_{m=0}^{2k-1} \frac{(x_i - \alpha)^m}{m!} \frac{\partial^m \mathbf{U}}{\partial x^m}(\alpha^-, t_n) + \mathcal{O}(\Delta x^{2k}), \quad (9)$$

and "on the right" of α ($i = J + 1, \dots, J + k$), with the jump conditions (5)

$$\begin{aligned} \mathbf{U}(x_i, t_n) &= \sum_{m=0}^{2k-1} \frac{(x_i - \alpha)^m}{m!} \frac{\partial^m \mathbf{U}}{\partial x^m}(\alpha^+, t_n) + \mathcal{O}(\Delta x^{2k}) \\ &= \sum_{m=0}^{2k-1} \frac{(x_i - \alpha)^m}{m!} \mathbf{f}_m \left(\mathbf{U}, \dots, \frac{\partial^{m+1} \mathbf{U}}{\partial x^{m+1}} \right) (\alpha^-, t_n) \\ &\quad + \mathcal{O}(\Delta x^{2k}). \end{aligned} \quad (10)$$

In (9) and (10), we replace $\mathbf{U}(x_i, t_n)$ by \mathbf{U}_i^n , and we confuse the exact limit values with their numerical estimations; we also remove the Taylor rests and $\frac{\partial^{2k} \mathbf{U}}{\partial x^{2k}}(\alpha^-, t_n)$. We get the following nonlinear system

$$\mathbf{F} \left(\mathbf{U}(\alpha^-, t_n), \dots, \frac{\partial^{2k-1} \mathbf{U}}{\partial x^{2k-1}}(\alpha^-, t_n) \right) = \mathbf{0}, \quad (11)$$

which depends on \mathbf{U}_i^n ($i = J - k + 1, \dots, J + k$). The $4k \times 4k$ system (11) is solved by the Newton method.

4 Numerical experiments

We consider a 400-m long domain, with a fracture at $\alpha = 200.67$ m, and realistic physical parameters [7]

$$\begin{cases} \rho_0 = \rho_1 = 1200 \text{ kg/m}^3, & K = 1.3 \cdot 10^9 \text{ kg/s}^2, \\ c_0 = c_1 = 2800 \text{ m/s}, & d = 6.1 \cdot 10^{-4} \text{ m}. \end{cases}$$

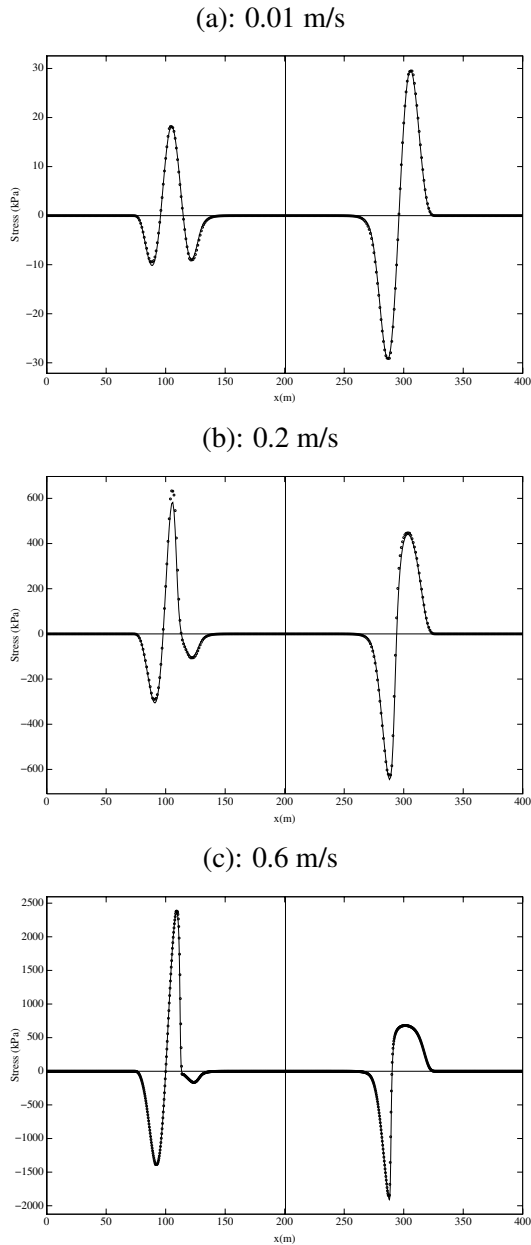


Figure 3: Numerical (...) and exact values (-) of σ , for three amplitudes of the incident velocity v .

The incident wave, initially on the left of α , is a spatially-bounded sinusoid, with a central frequency 50 Hz. In figure 3, three amplitudes of the incident velocity v are considered: 0.01 m/s (a), 0.2 m/s (b), and 0.6 m/s (c). The numerical solution is computed on 400 grid points (a-b) or 1200 grid points (c), with CFL=0.9 and $k = 2$ in (7). The analytical solution is computed by the method of characteristics [7]. The three snapshots are shown after the interaction of the incident wave with the fracture.

In (a), one could not distinguish the analytical solution

from the exact solution obtained in the linear case: the amplitude of the incident wave is insufficient to mobilize the nonlinearity of the fracture. The case (b) corresponds to realistic seismic waves in site investigation. Nonlinear effects are not negligible. The case (c) corresponds to blasting waves. Nonlinear effects are important, leading to shock-like waves. The numerical solution is computed on more grid points than for (a-b): otherwise, it does not converge to the exact solution. The reason may be that Taylor expansions (9)-(10) are inaccurate on a coarse grid when sharp fronts are near α .

5 Conclusion

This work is a preliminary attempt, and many things remain to be investigated. First, the existence, unicity, and regularity of the solution of (2)-(4) seem open questions. Second, it is essential to guarantee convergence towards the "good" solution of (11). A way may be to increase k in (9)-(10). Third, a similar study must be done on shear waves, satisfying other jump conditions with friction.

References

- [1] S.C. Bandis, A.C. Lumsden, N.R. Barton, "Fundamentals of rock fracture deformation", *Int. J. Rock Mech. Min. Sci. Geomech. Abstr.*, vol. 20-6, pp. 249-268, 1983.
- [2] R. J. LeVeque, "Wave propagation algorithms for multi-dimensional hyperbolic systems", *J. Comput. Phys.*, vol. 131, pp. 327-353, 1997.
- [3] B. Lombard, J. Piraux, "How to incorporate the spring-mass conditions in finite-difference schemes", *SIAM J. Scient. Comput.*, 24-4, pp. 1379-1407, 2003.
- [4] B. Lombard, J. Piraux, "Numerical treatment of 2D interfaces for acoustic and elastic waves", *J. Comput. Phys.*, vol. 195-1, pp. 90-116, 2004.
- [5] J. Piraux, B. Lombard, "A new interface method for hyperbolic problems with discontinuous coefficients: 1D acoustic example", *J. Comput. Phys.*, vol. 168-1, pp. 227-248, 2001.
- [6] L. Pyrak-Nolte, L. Myer, N. Cook, "Transmission of seismic waves across single natural fractures", *J. Geophys. Res.*, vol. 95-B6, pp. 8617-8638, 1990.
- [7] J. Zhao, J. G. Cai, "Transmission of elastic P-waves across single fractures with a nonlinear normal deformational behavior", *Rock Mech. Rock Engng.*, vol. 34-1, pp. 3-22, 2001.